

Existence and stability of regularized shock solutions, with applications to rimming flows

E. S. Benilov · M. S. Benilov · S. B. G. O'Brien

Received: 24 April 2007 / Accepted: 17 March 2008 / Published online: 5 April 2008
© Springer Science+Business Media B.V. 2008

Abstract This paper is concerned with regularization of shock solutions of nonlinear hyperbolic equations, i.e., introduction of a smoothing term with a coefficient ε , then taking the limit $\varepsilon \rightarrow 0$. In addition to the classical use of regularization for eliminating physically meaningless solutions which always occur in non-regularized equations (e.g. waves of depression in gas dynamics), we show that it is also helpful for stability analysis. The general approach is illustrated by applying it to rimming flows, i.e., flows of a thin film of viscous liquid on the inside of a horizontal rotating cylinder, with or without surface tension (which plays the role of the regularizing effect). In the latter case, the spectrum of available linear eigenmodes appears to be continuous, but in the former, it is discrete and, most importantly, remains discrete in the limit of *infinitesimally* weak surface tension. The regularized (discrete) spectrum is fully determined by the point where the velocity of small perturbations vanishes, with the rest of the domain, including the shock region, being unimportant.

Keywords Liquid films · Rimming flows · Shocks · Stability · Surface tension

1 Introduction

It is well-known that nonlinear hyperbolic PDEs (partial differential equations) admit shock solutions, i.e., solutions with discontinuities. The simplest such PDE describes unidirectional propagation of waves in a gas or shallow channel filled with liquid,

$$\frac{\partial h}{\partial t} + h \frac{\partial h}{\partial x} = 0, \quad (1)$$

where h is the nondimensional density of the gas or depth of the liquid, and x, t are the nondimensional coordinate and time. We shall seek steadily translating solutions, i.e.,

$$h = H(\xi), \quad \xi = x - vt, \quad (2)$$

E. S. Benilov · S. B. G. O'Brien (✉)
Department of Mathematics, University of Limerick, Limerick, Ireland
e-mail: stephen.obrien@ul.ie

M. S. Benilov
Department of Physics, University of Madeira, Funchal, Portugal

where v is the translation speed. Substitution of (2) into Eq. 1 yields $dH/d\xi = 0$, and shock solutions result from the assumption that H is a piecewise constant function, e.g.

$$H(\xi) = \begin{cases} H_- & \text{if } \xi < 0, \\ H_+ & \text{if } \xi > 0, \end{cases} \quad (3)$$

where H_+ and H_- are the amplitudes of the solution before and after the shock. Clearly, Eq. 1 is inapplicable at the point of discontinuity and, thus, provides no information regarding its dynamics. Instead, one usually resorts to ‘physically justified’ shock conditions—such as, for example, the Rankine–Hugoniot condition (e.g. [1, p. 24]), according to which the translation velocity is

$$v = \frac{1}{2} (H_- + H_+). \quad (4)$$

Observe that solution (2)–(4) formally exists for both $H_- < H_+$ and $H_- > H_+$ (i.e., for waves of depression and compression, respectively). It can be shown, however, that waves of depression do not satisfy the so-called causality principle (e.g. [1, p. 56]), which implies that they are meaningless physically.¹

The causality principle has also connections with *stability* of shock solutions. Solutions that satisfy it are stable, while the stability properties of those that do not are unclear, as the corresponding linearized problem is ill-posed (see [1, p. 324]). Still, even though the causality principle produces sensible results for both existence and stability of shock solutions, such an ‘axiomatic’ tool seems to be more relevant to basic physical theories rather than solutions of PDEs. One would expect to deal with the latter through mathematical, not physical means.

There is another application where shock solutions play an important role, namely, thin films (e.g. [3,4]) and, in particular, rimming flows [5–10]—i.e., flows of a thin film of viscous liquid on the inside of a horizontal rotating cylinder (see Fig. 1). The governing equation in this case is (see [11])

$$\frac{\partial h}{\partial t} + \frac{\partial}{\partial \theta} \left(h - \frac{1}{3} h^3 \cos \theta \right) = 0, \quad (5)$$

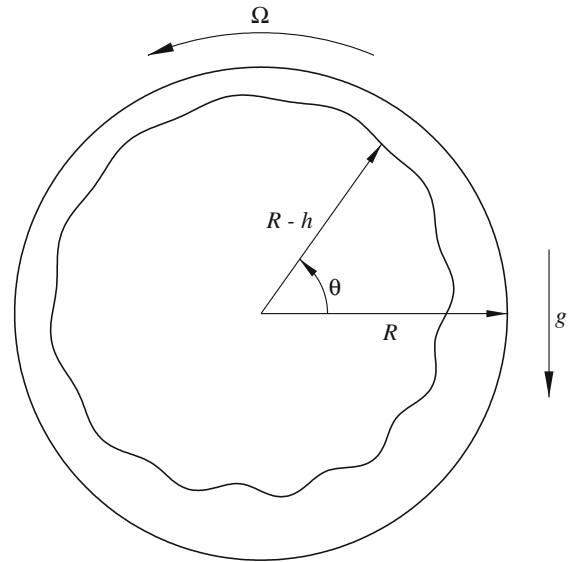
where h is the nondimensional thickness of the film, θ and t are the polar angle and nondimensional time. Equation 5 admits two types of shock solutions, with stationary shocks located in the first and fourth quadrants. The former type does not satisfy the causality principle and, thus, is physically meaningless [5,6], while a linear stability analysis of the latter yields a continuous spectrum of stable eigenmodes (solutions with exponential dependence on time) [7]. In addition to the discontinuity associated with the shock, higher derivatives of these eigenmodes may be singular at $\theta = 0$, and the requirement that they be regular reduces the continuous spectrum to a countable set [9]. It is unclear, however, why one should disregard seemingly legitimate eigenmodes, merely because their n th derivatives (with n being as large as one wants) misbehave at a single point.

The aim of the present work is two-fold. Firstly, we develop a tool for dealing with stability of shock solutions; secondly, we re-examine the rimming-flow problem and clarify the discrepancy between [7] and [9]. Both aims will be achieved through *regularization* [12,13], i.e., introduction of a smoothing term in the PDE in question. For Eq. 1, this will be a second-derivative term describing modelling viscous effects; and for (5), a combination of second, third, and fourth derivatives, modelling surface tension. Denoting the coefficients of the smoothing terms in each case by ε , we take the limit $\varepsilon \rightarrow 0$ and show that it yields solutions that automatically satisfy the causality principle (those that do not simply do not exist in the regularized equation). The same approach clarifies the stability properties of rimming flows: no matter how weak surface tension is, it discriminates between the results of [7] and [9].

This paper has the following structure. In Sect. 2, we illustrate the approach outlined above by regularizing Eq. 1. In Sect. 3, we examine the existence of shock solutions of the regularized version of Eq. 5 (governing rimming flows with surface tension); and in Sect. 4, we examine their stability.

¹ This conclusion can also be derived from the Lax entropy condition [2], which is an alternative means of eliminating physically meaningless solutions of nonlinear hyperbolic equations.

Fig. 1 Liquid film in a rotating horizontal cylinder



2 Regularization of Eq. 1

Introducing in (1) a second-derivative term (which, physically, describes viscosity), we obtain Burgers' equation,

$$\frac{\partial h}{\partial t} + h \frac{\partial h}{\partial x} - \varepsilon \frac{\partial^2 h}{\partial x^2} = 0, \quad (6)$$

which is very well studied [12–15] and, thus, provides a perfect testbed for our approach.

2.1 Steadily translating solutions

Steadily translating shock solutions of Burgers' equation (6) were examined, as a particular case, in [12, 13], and we shall not discuss them in detail. We shall only mention that substitution of (2) in (6) yields

$$\frac{d}{d\xi} \left(-vH + \frac{1}{2}H^2 - \varepsilon \frac{dH}{d\xi} \right) = 0.$$

Solving this ODE with the assumption that H is bounded as $\xi \rightarrow \pm\infty$, we obtain

$$H = v - a \tanh \left(\frac{a\xi}{2\varepsilon} \right), \quad (7)$$

where a is an arbitrary constant. It can be readily shown that, as $\varepsilon \rightarrow 0$, (7) tends to solution (2)–(3) with

$$H_+ = v - |a|, \quad H_- = v + |a|. \quad (8)$$

Thus, only those solutions of the original equation (1) that have $H_- \geq H_+$ follow from the $\varepsilon \rightarrow 0$ limit of the regularized equation (6). Furthermore, relationship (4) between H_{\pm} and the translation velocity v automatically follows from (8), i.e., regularization also justifies the Rankine–Hugoniot condition.

2.2 Stability

The stability properties of the solution (7) will be illustrated for the particular case of a stationary ($v = 0$) shock with $a = 1$,

$$H = -\tanh \left(\frac{x}{2\varepsilon} \right). \quad (9)$$

Let

$$h = H + \tilde{h}, \quad (10)$$

where \tilde{h} is a small perturbation. Substituting (10) in (6) and linearizing it, we obtain

$$\frac{\partial \tilde{h}}{\partial t} + H \frac{\partial \tilde{h}}{\partial x} + \tilde{h} \frac{\partial H}{\partial x} - \varepsilon \frac{\partial^2 \tilde{h}}{\partial x^2} = 0. \quad (11)$$

Now, recall that the Hopf–Cole transformation [14, 15],

$$h = -2\varepsilon \frac{\partial}{\partial x} \log u,$$

reduces Burgers' equation to the heat equation,

$$\frac{\partial u}{\partial t} - \varepsilon \frac{\partial^2 u}{\partial x^2} = 0. \quad (12)$$

In particular, $H(x)$ given by (9) corresponds to the solution $u = U(x, t)$ of (12) with

$$U = 2 \cosh\left(\frac{x}{2\varepsilon}\right) \exp\left(\frac{t}{4\varepsilon}\right).$$

It is natural to expect, and can be verified by inspection, that the *linearized* Hopf–Cole transformation

$$\tilde{h} = -2\varepsilon \frac{\partial}{\partial x} \left(\frac{\tilde{u}}{U} \right), \quad (13)$$

reduces the *linearized* Burgers equation (11) to the *linearized* version of (12). The latter is already linear, so we just replace u with \tilde{u} in it to obtain

$$\frac{\partial \tilde{u}}{\partial t} - \varepsilon \frac{\partial^2 \tilde{u}}{\partial x^2} = 0. \quad (14)$$

Now, apply transformation (13) to the following solution of (14):

$$\tilde{u} = -\frac{1}{4\varepsilon^2 k} \exp\left[\left(k + \frac{1}{2\varepsilon}\right)x + \varepsilon \left(k + \frac{1}{2\varepsilon}\right)^2 t\right], \quad (15)$$

where k is an arbitrary complex constant. The resulting solution of the linearized Burgers equation is

$$\tilde{h} = \left[\frac{1}{2} \exp\left(\frac{x}{2\varepsilon}\right) \sec\left(\frac{x}{2\varepsilon}\right) + \frac{1}{4\varepsilon k} \sec^2\left(\frac{x}{2\varepsilon}\right) \right] \exp\left[\left(\varepsilon k^2 + k\right)t + kx\right]. \quad (16)$$

To guarantee that \tilde{h} is bounded as $x \rightarrow \pm\infty$, one requires

$$-\frac{1}{\varepsilon} \leq \Re k \leq 0.$$

Similarly, one can obtain

$$\tilde{h} = \left[-\frac{1}{2} \exp\left(-\frac{x}{2\varepsilon}\right) \sec\left(\frac{x}{2\varepsilon}\right) + \frac{1}{4\varepsilon k} \sec^2\left(\frac{x}{2\varepsilon}\right) \right] \exp\left[\left(\varepsilon k^2 + k\right)t - kx\right], \quad (17)$$

with the same restriction on k . Most importantly, both solutions decay as $t \rightarrow +\infty$, which corresponds to asymptotic stability.

Observe also that (15) represents the general form of a solution with exponential dependence on time (eigenmode) of Eq. 14, on the basis of which one can show that (16)–(17) include *all* exponential solutions of the linearized Burgers equation. Thus, regularized shocks are asymptotically stable with respect to all existing eigenmodes.

In order to interpret solutions (16)–(17) physically, observe that, say, for (16),

$$\lim_{\varepsilon \rightarrow 0} \tilde{h} = \begin{cases} 0 & \text{for } x < 0, \\ e^{k(x+t)} & \text{for } x \geq 0, \end{cases}$$

where $\Re k \leq 0$. This solution describes a disturbance coming from $+\infty$ and being absorbed by the shock. Similarly, solution (17) describes a disturbance coming from $-\infty$ and, again, being absorbed by the shock. In both cases perturbations are absorbed *completely*; hence, the regions on opposite sides of the shock are, in a sense, disconnected, as no information can pass through the shock (this issue will be revisited in Sect. 4).

Thus, the regularized and non-regularized problems each admit a continuous spectrum of stable eigenmodes.

3 Existence of shocks in rimming flows

3.1 Flows without surface tension

For steady rimming flows, $h = H(\theta)$, Eq. 5 yields

$$H - \frac{1}{3}H^3 \cos \theta = q, \tag{18}$$

where the constant of integration q represents the non-dimensional flux due to entrainment of the liquid by the cylinder's rotation. This cubic equation was examined in [11], where it was demonstrated that, if $q < \frac{2}{3}$, Eq. 18 has a smooth unique solution; see Fig. 2a. For $q = \frac{2}{3}$, $h(\theta)$ has a 'corner' at $\theta = 0$; see Fig. 2b. Thus, there exists a family of steady rimming flows characterized by different values of the flux $q \leq \frac{2}{3}$.

Instead of q , however, it is more physical to characterize the solution by the non-dimensional net mass M , i.e., to solve (18) with an additional constraint,

$$\int_0^{2\pi} H \, d\theta = M. \tag{19}$$

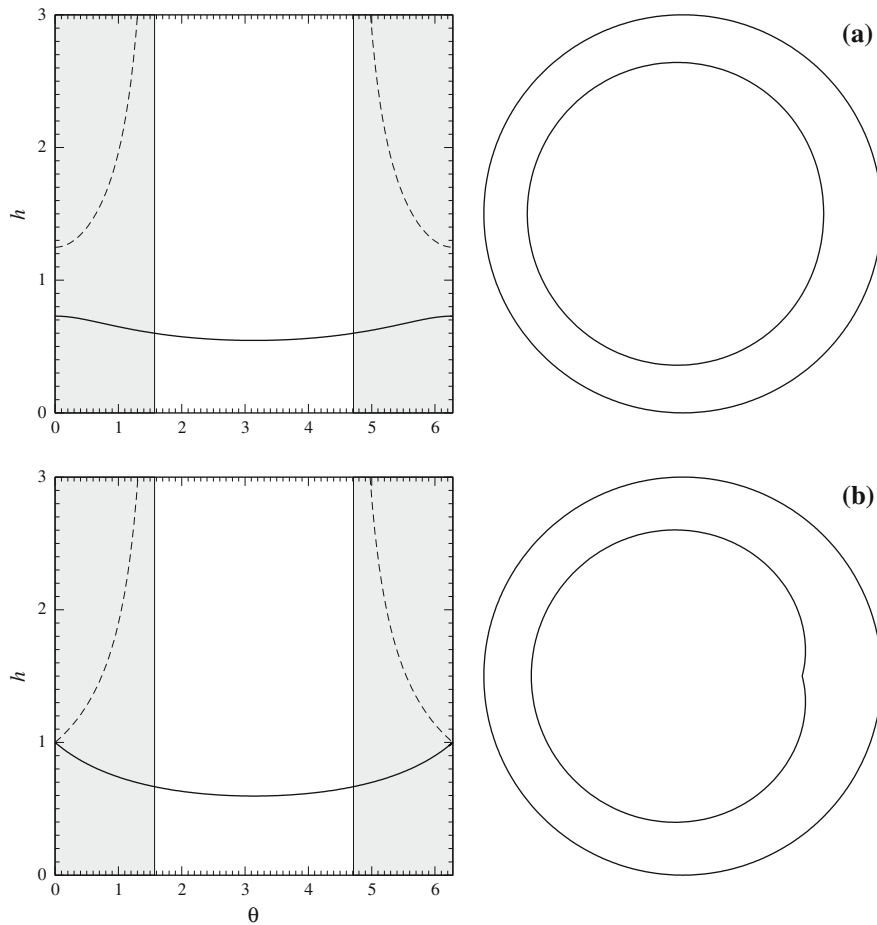


Fig. 2 Rimming flows with continuous profile. The left-hand panels show the solution in Cartesian coordinates (the solid/dashed line corresponds to the smaller/larger root of (18), the first and fourth quadrants are shaded). The right-hand panels show the solution in polar coordinates. **(a)** $q = 0.6$, **(b)** $q = \frac{2}{3}$

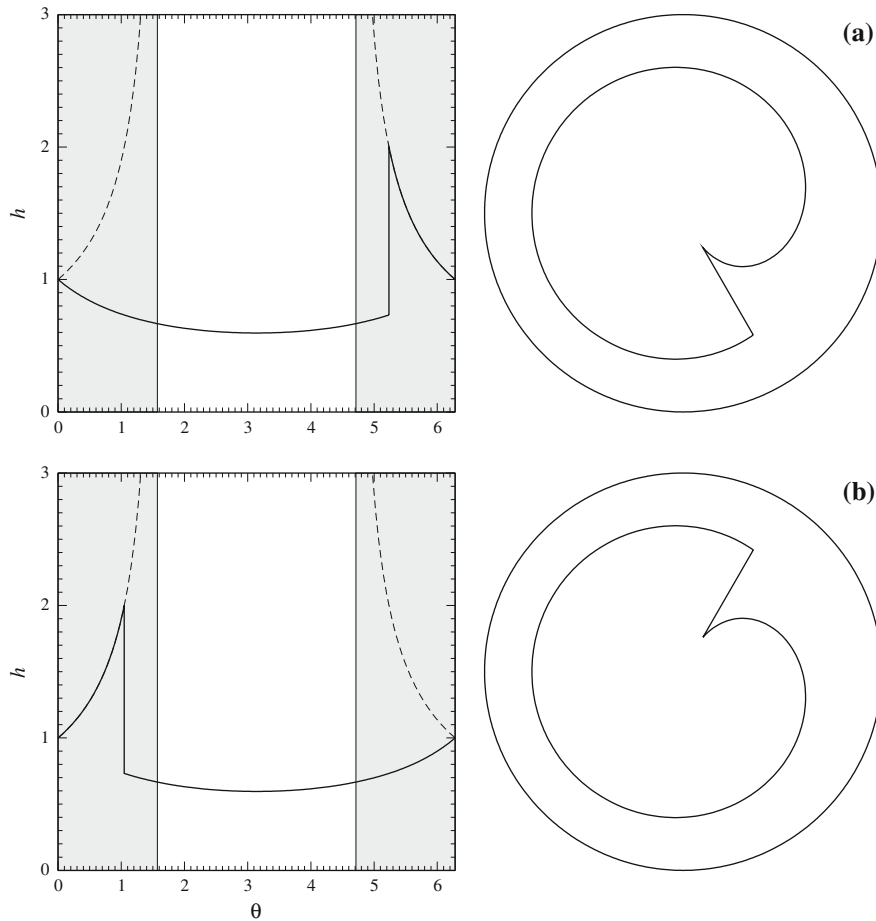


Fig. 3 Rimming flows with shocks. As in Fig. 2, the left-hand panels show the solution in Cartesian coordinates, the right-hand panels show the solution in polar coordinates. **(a)** The shock is located at $\theta = \frac{5}{3}\pi$ (in the fourth quadrant). **(b)** The shock is located at $\theta = \frac{1}{3}\pi$ (in the first quadrant)

The flux, in this case, should be treated as a function of the mass, $q(M)$. In particular, the limiting solution with $q = \frac{2}{3}$ corresponds to $M_* \approx 4.44$ (as computed via numerical integration of $H(\theta)$; see, for example, [6]).

Next, imagine that the actual mass of the liquid inside the cylinder exceeds the threshold value M_* . In this case, the film is no longer thin enough for viscous entrainment to ‘overcome’ gravity, and liquid parcels cannot climb past the point $\theta = 0$, where the tangent to the cylinder’s surface is vertical and gravity is, thus, the strongest. These parcels accumulate on the rising side of the cylinder, where the film becomes so thick that the liquid starts falling back and forms a shock, similar to that of a tidal bore [5,6]. Note that the shock’s position is determined by M , i.e., to accommodate a larger amount of liquid, the shock will be located closer to the bottom of the cylinder, and vice versa.

In order to understand the mathematical nature of the shock solutions, note that, in the first and fourth quadrants, Eq. 18 has two positive roots, with the smaller of the two corresponding to continuous solutions (see the left-hand panels of Fig. 2). For $q = \frac{2}{3}$, the two roots touch at $\theta = 0$ and allow for a continuous transition from the smaller root to the larger one (see the left-hand panels of Fig. 3). Observe that, as $\theta \rightarrow \frac{1}{2}\pi, \frac{3}{2}\pi$, the larger root becomes infinite; hence, the solution must ‘jump’ back to the smaller root before this occurs. As a result, solutions with shocks in the first and fourth quadrants are both possible; see Figs. 3a, b, respectively.

However, only the latter type is supported by the above intuitive argument based on liquid parcels. Furthermore, the former type does not satisfy the causality principle (see [5,6]) and, thus, is meaningless physically.

Finally, it can be shown that the net mass of shock solutions can never exceed a certain threshold value, $M_{**} \approx 6.93$; thus, initial conditions with $M > M_{**}$ appear to have no steady state to evolve to. We shall not discuss what happens in such cases in this paper, but mention only that they have been examined in [8, 10].

3.2 Rimming flows with surface tension

The simplest way to regularize Eq. 5 is to take into account surface tension,² which yields (e.g. [5, 8, 17])

$$\frac{\partial h}{\partial t} + \frac{\partial}{\partial \theta} \left(h - \frac{1}{3} h^3 \cos \theta \right) + \frac{\partial}{\partial \theta} \left[\frac{1}{3} \varepsilon h^3 \left(\frac{\partial h}{\partial \theta} + \frac{\partial^3 h}{\partial \theta^3} \right) \right] = 0, \quad (20)$$

where ε is a nondimensional parameter characterizing surface tension (for physical background of Eq. 20, see Appendix A). Note also that, in many applications, ε is small.

For steady solutions, $h = H(\theta)$, (20) yields

$$H - \frac{1}{3} H^3 \cos \theta + \frac{1}{3} \varepsilon H^3 \left(\frac{dH}{d\theta} + \frac{d^3 H}{d\theta^3} \right) = q, \quad (21)$$

where q is the nondimensional flux. This equation is to be solved with the periodicity condition,

$$H(\theta + 2\pi) = H(\theta). \quad (22)$$

The boundary-value problem (21)–(22) cannot be solved analytically, so we shall analyze it asymptotically for $\varepsilon \ll 1$.

First of all, recall that, for $\varepsilon = 0$ (no surface tension), all shock solutions correspond to $q = \frac{2}{3}$; hence, for small ε , we can safely assume $q \approx \frac{2}{3}$ (this assumption will be confirmed numerically later).

Observe also that, except for the shock region, surface tension can be neglected, and the solution is close to the one shown in Fig. 3.

To find the structure of the shock region, let it be located near θ_s . Rewriting (21) in terms of the ‘inner’ spatial variable³

$$x = \varepsilon^{-1/3} (\theta - \theta_s), \quad (23)$$

replacing q with its leading-order value $q = \frac{2}{3}$, and omitting small terms, we obtain

$$H - \frac{1}{3} H^3 \cos \theta_s + \frac{1}{3} H^3 \frac{d^3 H}{dx^3} = \frac{2}{3}. \quad (24)$$

To match the inner solution with the outer one, the following matching conditions must be imposed:

$$H \rightarrow H_{\pm} \quad \text{as } x \rightarrow \pm\infty, \quad (25)$$

where H_{\pm} are the two positive roots of the cubic equation

$$H_{\pm} - \frac{1}{3} H_{\pm}^3 \cos \theta_s = \frac{2}{3}. \quad (26)$$

Most importantly, if θ_s is in the first quadrant, then $H_- > H_+$ (see Fig. 3b); and, if θ_s is in the fourth quadrant, then $H_- < H_+$ (see Fig. 3a).

² Alternatively, (5) can be regularized by giving up the lubrication approximation in the vicinity of the shock, similar to the way the solution with a ‘corner’ (shown in Fig. 2b) was treated in [16]. We shall not discuss this matter in detail, but note only that, physically, such an approach should be used when the effect of gravity is stronger than that of surface tension.

³ The following scaling for θ has been suggested earlier in [6, 8].

Next, we shall prove that the boundary-value problem (24)–(26) does not have a solution for $H_- > H_+$. Multiply (24) by

$$\frac{1}{H^3} \frac{dH}{dx},$$

and integrate it with respect to x from $-\infty$ to $+\infty$. Integrating by parts and taking into account (25), we obtain

$$\frac{\varepsilon}{3} \int_{-\infty}^{\infty} \left(\frac{d^2H}{dx^2} \right)^2 dx = \frac{1}{H_+^2} \left(H_+ + \frac{1}{3} H_+^3 \cos \theta_s - \frac{1}{3} \right) - \frac{1}{H_-^2} \left(H_- + \frac{1}{3} H_-^3 \cos \theta_s - \frac{1}{3} \right). \tag{27}$$

Using (26), one can show that

$$\text{r.h.s. of (27)} = \frac{(H_+ - H_-)(1 - H_+ H_- \cos \theta_s)}{2H_- H_+}$$

and

$$H_+ H_- = \frac{1}{\cos \theta_s} - \frac{(H_+ - H_-)^2}{3}.$$

Accordingly, (27) becomes

$$\frac{\varepsilon}{3} \int_{-\infty}^{\infty} \left(\frac{d^2H}{dx^2} \right)^2 dx = \frac{(H_+ - H_-)^3 \cos \theta_s}{6H_- H_+}.$$

If $H_- > H_+$, the right- and left-hand sides of this equality are of opposite signs, which means that the boundary-value problem (24)–(26) has no solution in this case.

Thus, if the outer solution (described by the non-regularized equation) involves a shock in the first quadrant, the inner solution cannot be matched across the shock. We conclude that the regularized problem as a whole has no solutions with shocks in the first quadrant, and we do not have to resort to the causality principle to show that they are physically meaningless.

Unfortunately, the inner problem (24)–(26) does not have an obvious analytical solution and, thus, the structure of regularized shocks cannot be described analytically. Of course, Eqs. 24–26 can be solved numerically, but so can the exact problem, Eqs. 21, 22, and that is what we now do, using a numerical method developed in [10].

Firstly, solutions with a (regularized) shock occurring in the first quadrant have never arisen in our computations. Secondly, we examined the relationship between the net mass M and the flux q ; see Fig. 4. One can see, that the leading-order prediction that, for $M \gtrsim 4.44$, $q \approx \frac{2}{3}$ is a good approximation. Thirdly, we examine the dependence of the solution on ε (Fig. 5). Observe that surface tension generates a ‘dimple’ on the left-hand side of the shock and a ‘hump’ on its right-hand side. Interestingly, neither the depth of the dimple, nor the height of the hump tend to zero as $\varepsilon \rightarrow 0$, which can be interpreted as a kind of Gibbs phenomenon.

4 Stability of shocks in rimming flows

4.1 Flows without surface tension

To examine the steady state $H(\theta)$ for stability (see [7]), let $h = H + \tilde{h}$, where \tilde{h} is a small perturbation. Then, after linearization, the (non-regularized) Eq. 5 yields

$$\frac{\partial \tilde{h}}{\partial t} + \frac{\partial}{\partial \theta} (c \tilde{h}) = 0, \tag{28}$$

where

$$c(\theta) = 1 - H^2 \cos \theta \tag{29}$$

Fig. 4 The flux q vs. the net mass M , for $\epsilon = 10^{-3}$. The upper panel shows a blow-up of the region shaded in the lower panel (the dotted line corresponds to $q = \frac{2}{3}$)

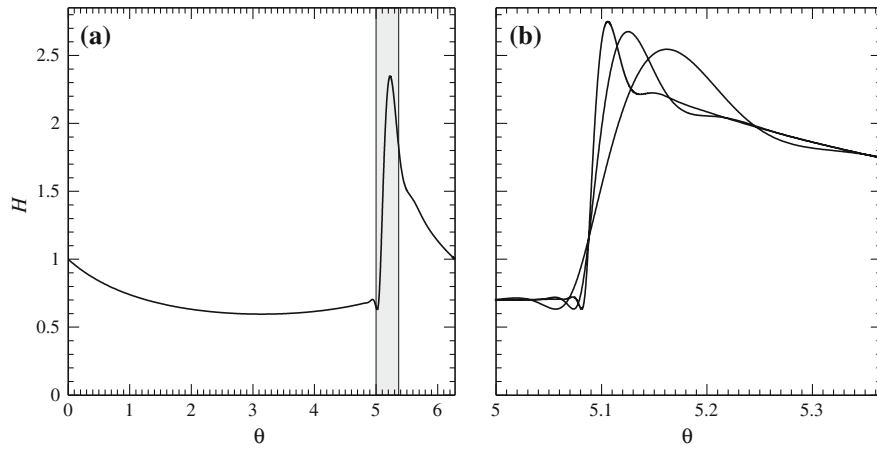
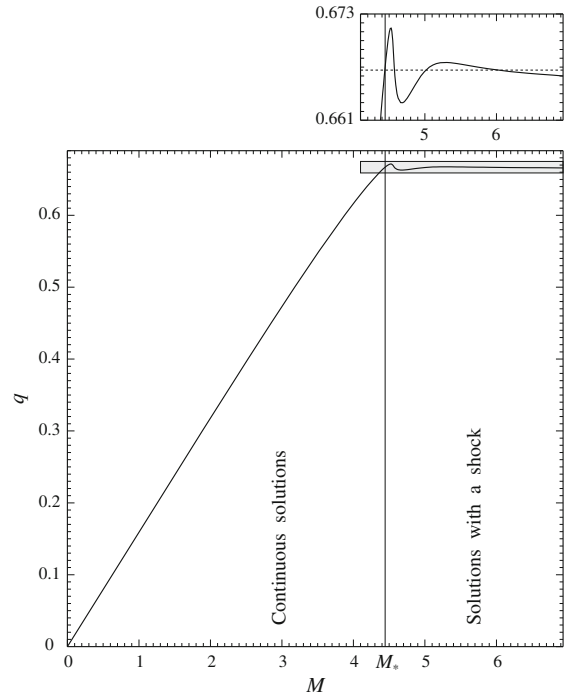


Fig. 5 Numerical solutions of Eq. 21. (a) $\epsilon = 10^{-4}$; (b) $\epsilon = 10^{-5}, 10^{-6}, 10^{-7}$ [smaller values of ϵ correspond to larger maxima of $H(\theta)$]. Panel (b) shows only the shock region, corresponding to the shaded area of panel (a). In all cases, the net mass of the solution is $M = 5.2$

is the local velocity of perturbations. We shall seek eigenmodes, i.e., solutions of the form

$$\tilde{h}(\theta, t) = \phi(\theta) e^{st},$$

for which (28) becomes

$$s\phi + \frac{d}{d\theta} (c\phi) = 0. \tag{30}$$

The general solution of this equation is

$$\phi = \frac{1}{c(\theta)} \exp \left[-s \int \frac{d\theta}{c(\theta)} \right]. \tag{31}$$

In what follows, we shall need the behavior of $c(\theta)$ at small θ . Equation 18 with $q = \frac{2}{3}$ yields three possible asymptotic solutions: one should choose the one that is positive and decays with growing θ (as it is the one that corresponds to the shock solution),

$$H(\theta) = 1 - \frac{1}{\sqrt{6}}\theta + O(\theta^2) \quad \text{as } \theta \rightarrow 0 \tag{32}$$

(this formula was originally obtained in [11] with a minor error, which was later corrected in [18]). Substituting (32) in (29), one can see that

$$c(\theta) = \sqrt{\frac{2}{3}}\theta + O(\theta^2) \quad \text{as } \theta \rightarrow 0. \tag{33}$$

Since c vanishes at $\theta = 0$, the integral in (31) diverges, and it is unclear how the eigenfunction should be extended across this point.

Physically, however, this issue is unimportant. Indeed, since perturbations have zero velocity at $\theta = 0$, they cannot pass through this point, nor can they pass through the shock. Thus, there are two ‘disconnected’ regions, $(0, \theta_s)$ and $(\theta_s, 2\pi)$, where the eigenfunction can be determined independently. Accordingly, the antiderivative can be assumed to satisfy

$$\int \frac{d\theta}{c(\theta)} \rightarrow \sqrt{\frac{3}{2}} \log \theta + A_{\pm} + O(\theta) \quad \text{as } \theta \rightarrow \pm 0, \tag{34}$$

with two independent complex constants A_- and A_+ . Equations (31), (33)–(34) fully determine the eigenfunction $\phi(\theta)$.

Next, it follows from (31), (33)–(34) that

$$\phi = -\sqrt{\frac{3}{2}}\theta^{-\sqrt{\frac{3}{2}}s-1}e^{A_{\pm}} + O\left(\theta^{-\sqrt{\frac{3}{2}}s}\right) \quad \text{as } \theta \rightarrow \pm 0. \tag{35}$$

Following [7], we require ϕ to be continuous as $\theta \rightarrow 0$, hence,

$$\Re s < -\sqrt{\frac{2}{3}}.$$

Since the real part of s is negative, all eigenmodes decay as $t \rightarrow \infty$; hence, the steady state is stable.

Observe, however, that if

$$-2\sqrt{\frac{2}{3}} < \Re s < -\sqrt{\frac{2}{3}}.$$

Equation 35 shows that $d\phi/d\theta$ and all further derivatives become infinite as $\theta \rightarrow 0$. An obvious way to ‘weaken’ the singularity is to make $\Re s$ smaller, say,

$$-3\sqrt{\frac{2}{3}} < \Re s < -2\sqrt{\frac{2}{3}}.$$

In this case, $d\phi/d\theta$ becomes finite, but $d^2\phi/d\theta^2$ and further derivatives are still infinite. In fact, to eliminate singularities in *all* derivatives, one has to choose, as suggested in [9],

$$s = -n\sqrt{\frac{2}{3}}, \tag{36}$$

where n is a non-negative integer, and also assume

$$A_+ = A_-. \tag{37}$$

An example of an eigenfunction satisfying (36)–(37) is shown in Fig. 6. One can see that ϕ is smooth at $\theta = 0$ (but still discontinuous at $\theta = \theta_s$).

We emphasize that the causality principle, or any other physical argument, *cannot* justify conditions (36)–(37). It turns out, however, that regularization by surface tension does just that.

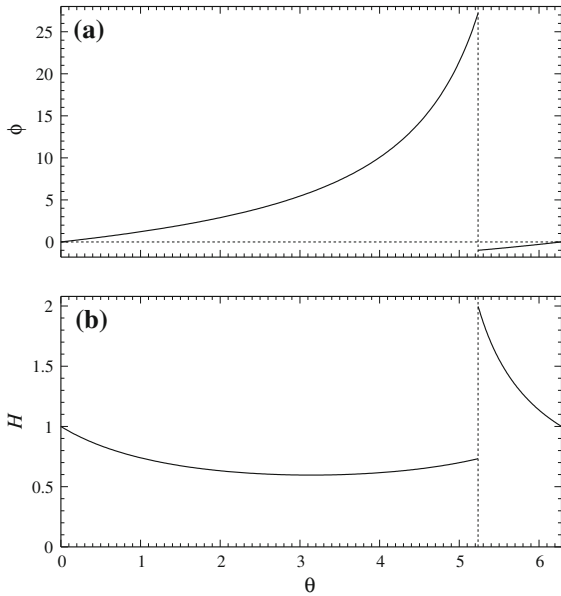


Fig. 6 A solution of the leading-order stability problem. (a) The eigenfunction determined by (31), (33)–(34), (36)–(37) with $n = 1$, and (b) the corresponding steady-state solution (the shock is located at $\theta_s = \frac{5}{3}\pi$)

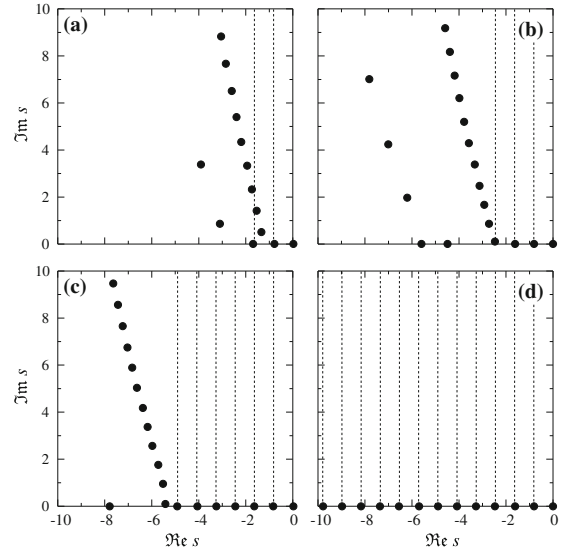


Fig. 7 The eigenvalues of problem (38)–(39) for the steady state with $M = 5.2$. (a) $\varepsilon = 10^{-4}$, (b) $\varepsilon = 10^{-5}$, (c) $\varepsilon = 10^{-6}$, (d) $\varepsilon = 10^{-7}$. The dotted line shows eigenvalues (36)

4.2 Rimming flows with surface tension

With surface tension included, Eq. 30 becomes

$$s\phi + \frac{d}{d\theta} \left[c\phi + \varepsilon H^2 \phi \left(\frac{dH}{d\theta} + \frac{d^3 H}{d\theta^3} \right) + \frac{1}{3} \varepsilon H^3 \left(\frac{d\phi}{d\theta} + \frac{d^3 \phi}{d\theta^3} \right) \right] = 0, \tag{38}$$

where the steady state $H(\theta)$ satisfies (21) and $c(\theta)$ is defined by (29). Equation 38 is to be solved with the periodicity condition

$$\phi(\theta + 2\pi) = \phi(\theta). \tag{39}$$

Equations (38)–(39) turn out to have a solution for *discrete* values of s , which will be referred to as the eigenvalue, with $\phi(\theta)$ being the eigenfunction. This result comes as no surprise, as regular problems with periodic boundary conditions normally have discrete spectra. This, however, does not prove that the spectrum of the non-regularized problem is also discrete. Indeed, as $\varepsilon \rightarrow 0$, the distance between neighboring eigenvalues of the latter problem may tend to zero, and the limiting spectrum may be continuous.

Since problem (38)–(39) is real, the eigenvalues occur in complex conjugate pairs. Note also that there always exists a zero eigenvalue $s = 0$, corresponding to an infinitesimal change of the flux q (or, equivalently, the mass M). Indeed, differentiating (21) with respect to q , one can see that the resulting equation is equivalent to (38) with

$$s = 0, \quad \phi = \frac{\partial H}{\partial q}.$$

To find other eigenvalues, problem (38)–(39) was solved numerically using the method described in Appendix B. Typical results are shown in Fig. 7: one can see that, as $\varepsilon \rightarrow 0$, the eigenvalues tend to (36), i.e., to those predicted in [9].

To interpret this result physically, recall that, for Burgers’ equation, regularization of the shock leaves the spectrum of eigenmodes exactly as it was, i.e., continuous. Therefore, the shock is unlikely to be responsible for the emergence

of the discrete spectrum in the rimming-flow problem. The only possible reason, in fact, is the regularization of the region near $\theta = 0$, where the leading-order solution has a singularity as well.

Thus, we need to analyze the eigenvalue problem (38)–(39) for small θ . To do so, replace H and c with their small- θ expansions (32)–(33), and replace q with its leading-order value, $q \approx \frac{2}{3}$. Then, in terms of an appropriate inner variable,

$$x = \varepsilon^{-1/4}\theta,$$

Eq. 38 becomes (small terms omitted)

$$\frac{d}{dx} \left(\frac{1}{3} \frac{d^3\phi}{dx^3} + \frac{2x}{\sqrt{6}}\phi \right) + s\phi = 0. \tag{40}$$

In order to set proper boundary conditions for this equation, we need to examine behavior of ϕ as $x \rightarrow \pm\infty$. It can be verified by inspection that one of the four linearly independent solutions of (40) behaves algebraically,

$$\phi \rightarrow x^{-\sqrt{\frac{3}{2}}s-1} \text{ as } x \rightarrow \pm\infty.$$

This solution matches the behavior of the outer solution [see (35)], and ϕ should certainly ‘include’ it.

The other three linearly independent solutions behave exponentially, and their large-distance asymptotics can be found using a WKB-type expansion (see Appendix C). It turns out that two out of the three solutions grow as $x \rightarrow \pm\infty$ and, thus, should be discarded, with the remaining one being

$$\phi \rightarrow x^{1+\frac{1}{\sqrt{6}}s} \exp\left(-3^{7/6}2^{-11/6}x^{4/3}\right) \text{ as } x \rightarrow \pm\infty. \tag{41}$$

This linearly independent solution should also be included in ϕ , i.e., the full boundary condition for (40) is

$$\phi \rightarrow B_{\pm}x^{-\sqrt{\frac{3}{2}}s-1} + D_{\pm}x^{1+\frac{1}{\sqrt{6}}s} \exp\left(-3^{7/6}2^{-11/6}x^{4/3}\right) \text{ as } x \rightarrow \pm\infty, \tag{42}$$

where B_{\pm} and D_{\pm} are undetermined constants. Observe that, due to the linearity of the problem, one of the constants can be equated to unity; hence, we have only *three* degrees of freedom for a *fourth*-order equation. As a result, (40), (42) have a solution only for special values of s , which makes s an eigenvalue.

Problem (40), (42) has been solved numerically by ‘shooting’, and the numerical eigenvalues agreed with (36) to an extremely high accuracy. Furthermore, B_+ and B_- turned out to be equal; hence, the matching of (42) to the outer solution (35) makes the corresponding constants in the latter, A_+ and A_- , equal as well. Thus, the regularized problem justifies assumption (37).

Note that, even though the ‘local’ equation (40) does not seem to have analytical solutions in the general case, if s assumes one of the values (36), it miraculously does! For $n = 0, 1, 2, 3$, for example, one can verify by inspection that the solution is simply

$$\phi = Bx^n, \tag{43}$$

where B is an arbitrary constant. Then, for $n = 4, 5, 6, 7$,

$$\phi = B \left[x^n + \frac{n!}{4\sqrt{6}(n-4)!}x^{n-4} \right], \tag{44}$$

and, for $n = 8, 9, 10, 11$,

$$\phi = B \left[x^n + \frac{n!}{4\sqrt{6}(n-4)!}x^{n-4} + \frac{n!}{192(n-8)!}x^{n-8} \right], \tag{45}$$

etc. As expected, in all these cases the boundary condition (42) is satisfied with $B_- = B_+$.

We emphasize that the above analytical solutions may not necessarily constitute the full spectrum (as, in principle, there can be other eigenvalues), which is why we needed to solve the problem numerically. Equations 43–45 should rather be viewed as a confirmation of the numerical results.

Finally, note that the limiting spectrum is independent of how exactly the equation for rimming flows is regularized. To illustrate this, we used a model suggested in [11],

$$\frac{\partial h}{\partial t} + \frac{\partial}{\partial \theta} \left(h - \frac{1}{3} h^3 \cos \theta \right) - \varepsilon \frac{\partial^2 h}{\partial \theta^2} = 0 \quad (46)$$

(which can be obtained by replacing in (20) the *fourth*-order (surface-tension) term with a *second*-order term). The steady states of (46) have been examined for stability and, as expected, the corresponding limiting (as $\varepsilon \rightarrow 0$) spectrum turned out to be exactly as (36). Indeed, analogous to (40), the small- θ equation in this case is

$$\frac{d}{dx} \left(-\frac{d\phi}{dx} + \frac{2x}{\sqrt{6}} \phi \right) + s\phi = 0.$$

Then, it can be readily verified that, even though the eigenfunctions of this equation differ slightly from (43)–(45), the corresponding eigenvalues are exactly the same as those of the (‘properly’ regularized) Eq. 40.

Furthermore, one can verify that smoothing by *any* even-ordered derivative would yield the same set of eigenvalues. One only has to make sure that the sign of the smoothing term corresponds to diffusion, not ‘anti-diffusion’. Odd-ordered derivatives, on the other hand, are unlikely to be suitable for regularization, as they often give rise to oscillations.

5 Concluding remarks

Thus, we have examined the existence and stability of shock solutions of nonlinear hyperbolic PDEs and their connection to regularization (i.e., introduction of a smoothing term with a small coefficient ε , then taking the limit $\varepsilon \rightarrow 0$). As expected, regularization filters out physically meaningless solutions, such as waves of depression in gas dynamics, and, in this respect, is equivalent to the causality principle.

In addition, regularization delivers important results that *cannot* be obtained using the causality principle.

Firstly, some hyperbolic PDEs have singularities associated with points where the local velocity of small perturbations vanishes, and it is unclear how these singularities affect the spectrum of linear eigenmodes. If, however, a smoothing term is inserted in the equation, the singularity disappears and the structure of the spectrum becomes clear. Eventually, one can take the limit of *infinitesimally* weak smoothing—and, thus, find out what happens in the original (non-smoothed) problem.

Secondly, even though the limiting results are independent of the specific form of the smoothing term, one should always use regularization by a *physically relevant* effect. This way, not only will the properties of the original solutions be clarified, but one will also find out how they are affected by a physically important influence.

Neither of the above results can be obtained using the causality principle.

The approach described has been applied to linear stability of rimming flows with shocks. It has been shown that the spectrum of the regularized (by surface tension) stability problem is discrete and fully determined by the point of zero velocity of small perturbations, whereas the rest of the domain, including the shock region, has no influence on the eigenvalues.

Finally, note that our analysis of the stability of rimming flows did not take into account the effect of inertia (associated with the material derivatives in the Navier–Stokes equations). Given that inertia has been shown to destabilize smooth rimming flows [17], it may destabilize shock solutions as well; this question requires further study.

Acknowledgement E. B. and S. O’B. acknowledge the support of the Mathematics Applications Consortium for Science and Industry (<http://www.macsi.ie>) funded by the Science Foundation Ireland, Mathematics Initiative grant 06/MI/005.

Appendix A: Physical background of Eq. 20

First of all, the variables h , θ , and t are related to their dimensional analogues (labelled with subscripts dim) by

$$h = \frac{h_{\text{dim}}}{\alpha R}, \quad \theta = \theta_{\text{dim}}, \quad t = \Omega t_{\text{dim}}, \quad (47)$$

where

$$\alpha = \left(\frac{\nu \Omega}{g R} \right)^{1/2}, \quad (48)$$

and g , ν , R , and Ω are the acceleration due to gravity, the liquid's kinematic viscosity, the cylinder's radius and angular velocity. The coefficient ε , in turn, is

$$\varepsilon = \frac{\sigma}{\rho g R^2} \left(\frac{\nu \Omega}{g R} \right)^{1/2},$$

where ρ and σ are the liquid's density and surface tension.

Equation 20 can be derived from the Stokes set using the standard lubrication approach (e.g. [5, 8, 17]), which assumes that the film is thin and its slope is small, i.e.,

$$h_{\text{dim}} \ll R, \quad \frac{\partial h_{\text{dim}}}{\partial \theta_{\text{dim}}} \ll 1.$$

In terms of the nondimensional variables (47), these conditions amount to

$$\alpha h \ll 1, \quad \alpha \frac{\partial h}{\partial \theta} \ll 1. \quad (49)$$

These conditions are most restrictive near the shock, where the film's thickness is largest and its slope, steepest. Accordingly, using the inner scaling (23) to estimate

$$h = O(1), \quad \frac{\partial h}{\partial \theta} = O(\varepsilon^{-1/3}), \quad \frac{\partial^2 h}{\partial \theta^2} = O(\varepsilon^{-2/3}), \dots, \quad (50)$$

one can reduce conditions (49) to a single inequality,

$$\alpha \ll \varepsilon^{1/3}. \quad (51)$$

(51) can be rewritten in terms of the volume fraction F , i.e., the ratio of the volume occupied by the liquid to that of the whole cylinder. Estimating

$$F \sim \frac{h_{\text{dim}}}{R} = \alpha h, \quad (52)$$

and recalling that, for shock solutions, $h = O(1)$, one can see that (51)–(52) imply

$$F \ll \varepsilon^{1/3}.$$

This restriction is slightly more stringent than the usual lubrication assumption $F \ll 1$.

Appendix B: Numerical solution of (38)–(39)

The eigenvalue problem (38)–(39) was treated using two different methods.

As the simplest approach, (38)–(39) were discretized (using second-order approximations of the derivatives on a mesh with a variable step), and its eigenvalues were computed using the LAPACK subroutine DGEEV (designed for finding the eigenvalues of large symmetric matrices; see [20]). It turned out, however, that this method works reasonably well only for $\varepsilon \gtrsim 10^{-5}$.

For smaller values of ε , we had to look for each eigenvalue individually, using the so-called relaxation (Newton linearization); see [19, Sect. 17.3]. Accordingly, (38)–(39) were replaced with

$$s_n \phi_n + (s_{n+1} - s_n) \phi_n + s_n (\phi_{n+1} - \phi_n) + \frac{d}{d\theta} \left[c \phi_n + \varepsilon H^2 \phi_n \left(\frac{dH}{d\theta} + \frac{d^3 H}{d\theta^3} \right) + \frac{1}{3} \varepsilon H^3 \left(\frac{d\phi_n}{d\theta} + \frac{d^3 \phi_n}{d\theta^3} \right) \right] = 0, \quad (53)$$

$$\phi_{n+1}(\theta + 2\pi) = \phi_{n+1}(\theta), \quad (54)$$

where (s_n, ϕ_n) represent the ‘current’ iteration and (s_{n+1}, ϕ_{n+1}) , the next one. Equation 53 was discretized using suitable second-order approximations of the derivatives on a mesh with a variable step (with smaller steps in the shock region). Then problem (53)–(54) was solved for (s_{n+1}, ϕ_{n+1}) using the LAPACK subroutine DGESV (designed for solving large sets of linear non-homogeneous equations; see [20]).

Appendix C: Far-field asymptotics for Eq. 40

Let

$$\phi = \exp \left(\int S dx \right), \quad (55)$$

where $S(\theta)$ is a new unknown. Substitution of (55) in (40) yields

$$\frac{d^3 S}{dx^3} + 3 \left(\frac{dS}{dx} \right)^2 + 4S \frac{d^2 S}{dx^2} + 6S^2 \frac{dS}{dx} + S^4 + \sqrt{6}(xS + 1) + 3s = 0. \quad (56)$$

Consider the limit $x \rightarrow \infty$ and seek a solution in the form

$$S = S_0 + S_1 + \dots \quad (57)$$

To leading order, (56) yields

$$S_0^4 + \sqrt{6}xS_0 = 0,$$

which admits three solutions

$$S_0 = -(\sqrt{6}x)^{1/3}, \left(\frac{1}{2} + \frac{\sqrt{3}i}{2} \right) (\sqrt{6}x)^{1/3}, \left(\frac{1}{2} - \frac{\sqrt{3}i}{2} \right) (\sqrt{6}x)^{1/3}.$$

ϕ must be bounded as $x \rightarrow \pm\infty$, which is the case only for

$$S_0 = -(\sqrt{6}x)^{1/3}. \quad (58)$$

In the next-to-leading order, (56) yields

$$6S_0^2 \frac{dS_0}{dx} + 4S_0^3 S_1 + \sqrt{6}xS_1 + \sqrt{6} + 3s = 0,$$

the solution of which is

$$S_1 = \left(1 + \frac{s}{\sqrt{6}} \right) \frac{1}{x}. \quad (59)$$

Substituting (57)–(59) in (55) and carrying out integration, we obtain

$$\phi \rightarrow \exp \left[-\frac{6^{1/6} 3}{4} x^{4/3} + \left(1 + \frac{s}{\sqrt{6}} \right) \log x \right] \quad \text{as } x \rightarrow \pm\infty,$$

which is equivalent to (41).

References

1. Ockendon JR, Howison SD, Lacey AA, Movchan AB (2003) Applied partial differential equations. Oxford University Press, Oxford
2. Lax PD (1957) Hyperbolic conservation laws II. *Comm Pure Appl Math* 10: 537–566
3. Bertozzi AL, Münch A, Fanton X, Cazabat AM (1998) Contact line stability and “undercompressive shocks” in driven thin film flow. *Phys Rev Lett* 81:5169–5172
4. Bertozzi AL, Münch A, Shearer M (1999) Undercompressive shocks in thin film flows. *Phys D* 134:431–464
5. Benjamin TB, Pritchard WG, Tavener SJ (1993) Steady and unsteady flows of a highly viscous liquid inside a rotating horizontal cylinder (unpublished, can be obtained from the authors of the present paper on request)
6. O’Brien SBG, Gath EG (1998) The location of a shock in rimming flow. *Phys Fluids* 10:1040–1042
7. O’Brien SBG (2002) A mechanism for two dimensional instabilities in rimming flow. *Q Appl Math* 60:283–300
8. Ashmore J, Hosoi AE, Stone HA (2003) The effect of surface tension on rimming flows in a partially filled rotating cylinder. *J Fluid Mech* 479:65–98
9. Acrivos A, Jin B (2004) Rimming flows within a rotating horizontal cylinder: asymptotic analysis of the thin-film lubrication equations and stability of their solutions. *J Eng Math* 50:99–121
10. Benilov ES, Benilov MS, Kopteva N (2007) Steady rimming flows with surface tension. *J Fluid Mech* 597:91–118
11. Moffatt HK (1977) Behaviour of a viscous film on the outer surface of a rotating cylinder. *J Mec* 16:651–673
12. Ladyzhenskaya OA (1957) On the construction of discontinuous solutions of quasi-linear hyperbolic equations as limits of solutions of the corresponding parabolic equations when the ‘coefficient of viscosity’ tends towards zero. *Proc Mosc Math Soc* 6:465–480 (in Russian)
13. Oleinik OA (1957) Discontinuous solutions of nonlinear differential equations. *Usp Mat Nauk* 12:3–73
14. Hopf E (1950) The partial differential equation $u_t + uu_x = \mu u_{xx}$. *Comm Pure Appl Math* 3:201–230
15. Cole JD (1951) A quasi-linear parabolic equation in aerodynamics. *Quart Appl Math* 9:225–236
16. Wilson SK, Hunt R, Duffy BR (2002) On the critical solutions in coating and rimming flow on a uniformly rotating horizontal cylinder. *Q J Mech Appl Math* 55:357–383
17. Benilov ES, O’Brien SBG (2005) Inertial instability of a liquid film inside a rotating horizontal cylinder. *Phys Fluids* 17:052106 (16 pp)
18. Duffy BR, Wilson SK (1999) Thin-film and curtain flows on the outside of a rotating horizontal cylinder. *J Fluid Mech* 394:29–49
19. Press WH, Teukolsky SA, Vetterling WT, Flannery BP (1992) Numerical recipes, 2nd ed. Cambridge University Press, Cambridge
20. LAPACK—Linear Algebra PACKage, <http://www.netlib.org/lapack>